Whitepaper
From single cells to complex 3D environments

January, 2024 For Research Use Only. Not for use in diagnostic procedures.

Uncovering high-resolution mechanical testing across scales

by Optics11 Life   January, 2024

© 2024 Optics11 Life B.V.

Mechanical properties can influence cellular fate across scales, from single-cell mechanics to the bulk mechanics of 3D cellular environments. However, accessing the mechanical properties of extensive areas at high resolution poses a challenge when relying on conventional mechanical characterization techniques. This white paper discusses the applications of Optics11 Life's unique technology in conducting precise mechanical testing across multiple length scales and resolutions on a wide range of biological samples.

INTRODUCTION

The mechanical properties of biological samples and biomaterials reveal valuable knowledge about their behavior and function. The characterization of material mechanical properties at cell and tissue length scales is becoming increasingly relevant in medical and life sciences, mainly because the mechanics of cells and their microenvironment regulate various biological processes[1].

Mechanical properties can be probed across scales, from single cells to complex 3D cellular systems. However, for the mechanical characterization of extensive areas at high resolution, conventional methods, such as atomic force microscopy (AFM) and rheometry, encounter challenges. AFM can only measure small sample areas, restricting its application to localized testing on the cellular and subcellular scales. Rheometry, on the other hand, measures bulk properties and may overlook local variation within a sample[2,3].

To address the needs of mechanobiology, Optics11 Life developed novel types of indenters to measure large areas of a wide range of biological samples, including cells, tissues, spheroids, organoids, and biomaterials, with high spatial resolution. This technology allows the probing of properties across broad scales, from 1 to over 200 μm of contact area, and the continuous mapping of properties over large areas, up to tens of cm^2. This is especially crucial when dealing with heterogeneous materials or complex structures, where different regions may possess distinct mechanical properties.

This white paper reviews studies on the mechanical characterization across multiple length scales and resolutions of a wide variety of biological samples using Optics11 Life technology.

INDENTATION PROBES: WHY TIP SIZE MATTERS

At the center of Optics11 Life technology are our pre-aligned, reusable, and pre-calibrated fiber optic probes. Probes are equipped with spherical tips ranging from 3 to 250 μm of radius (Figure 1). This broad range of dimensions allows the user to select the resolution of the measurement, adapting it to the sample and the experimental question. The bigger tips are ideal for measuring bulk mechanical properties over a relatively large area and avoiding the effects of irregularities on rough surfaces. Moreover, they allow indenting the sample at greater depths, accessing the mechanical characteristics of deeper layers. On the other end of the size range, smaller tips offer higher resolution and the possibility to distinguish topological and mechanical heterogeneities at a fine scale while still allowing for large-area mapping. Additionally, to optimize the testing of non-flat samples, the smaller tips (3–25 μm radius) are separated from the cantilever by a 30–100 μm rod extension. Importantly, Optics11 life probes measure even the softest materials with high force resolution in a non-destructive manner.
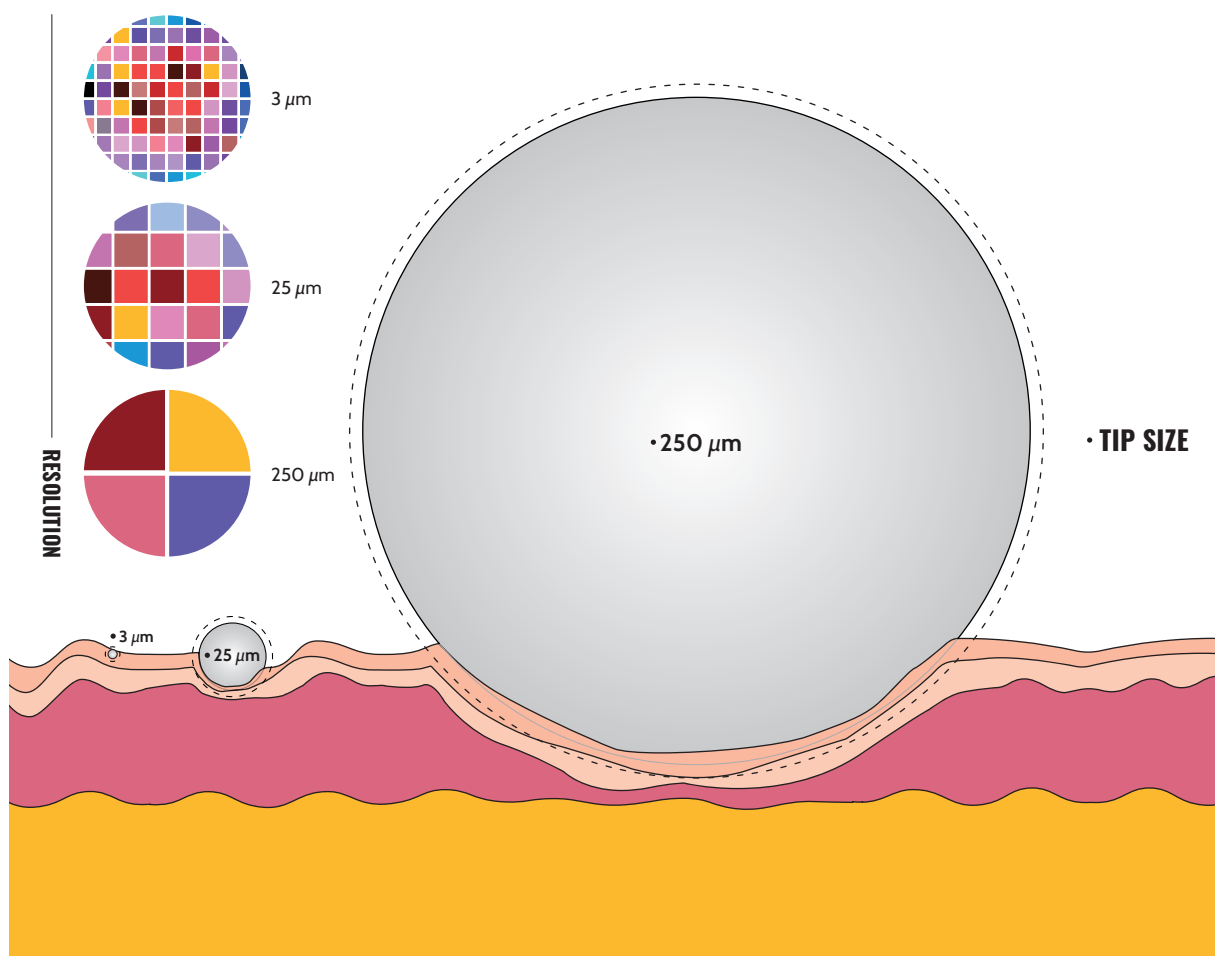
› **Figure 1**

The scale of mechanical testing. Illustration of three tip sizes on the tissue surface. The choice of tip determines mapping resolution. Large tips can measure bulk properties over large areas, minimizing the effect of irregularities on rough surfaces. Meanwhile, smaller tips offer higher resolution and can distinguish topological and mechanical heterogeneities at a fine scale.

INTRACELLULAR AND INTERCELLULAR SPATIAL RESOLUTION IN 2D CULTURES

The mechanical properties of living cells, such as their stiffness and viscoelasticity, regulate cellular function, behavior, and physical interactions with the surrounding extracellular matrix. Changes in cell mechanical properties impact numerous cellular activities, including cell adhesion, migration, polarization, differentiation, organelle organization, and trafficking inside the cytoplasm[4,5,6].

Mechanical tension plays a pivotal role in cellular dynamics, whether arising from the cell's cytoskeleton or applied externally to the cell surface. This tension can influence various cellular components, including the membrane, nucleus, and other organelles. The intricate interplay of mechanical forces extends beyond the confines of single cells, affecting the cell-cell contact area and the extracellular environment[7].
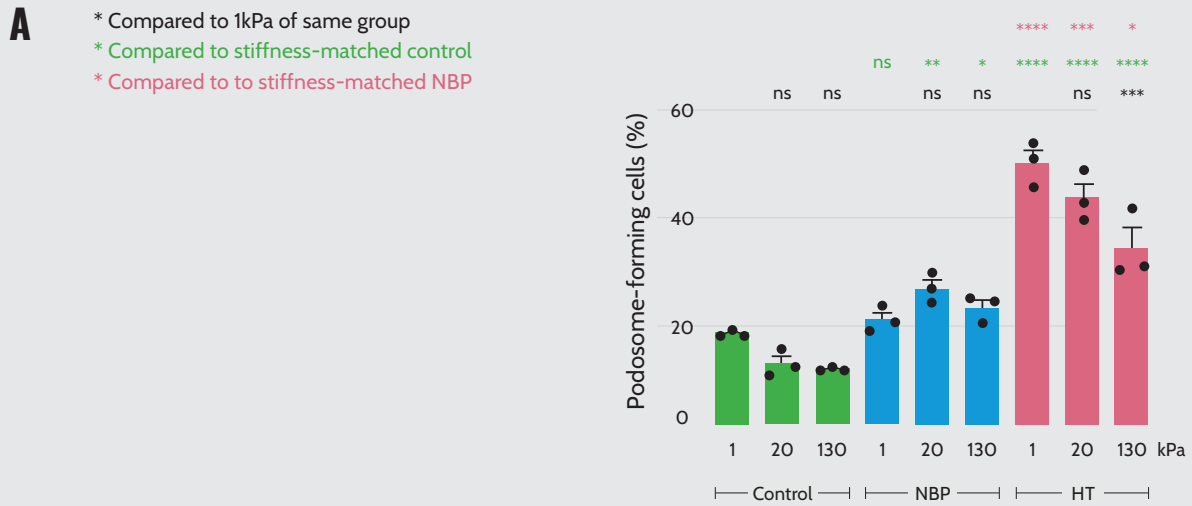
In the pursuit of elucidating the mechanical properties of cellular structures, Optics11 Life nanoindenters offer a high-resolution approach to investigating the mechanics of 2D cell cultures at the microscale. This sophisticated method allows researchers to delve into the intricate mechanical dynamics of living cells, offering valuable knowledge of how mechanical changes affect cellular processes.

To evaluate the impact of the local mechanical environment on single cells, Swiatwloaska et al.[8] performed nanoindentation measurements on the nucleus. They investigated how the stiffness of the extracellular matrix and simulated blood pressure affect vascular smooth muscle cells (VSMCs) involved in the progression of atherosclerosis. Also, they examined the calcium response through pressure stimulation of cells using a controlled force applied by the nanoindenter.
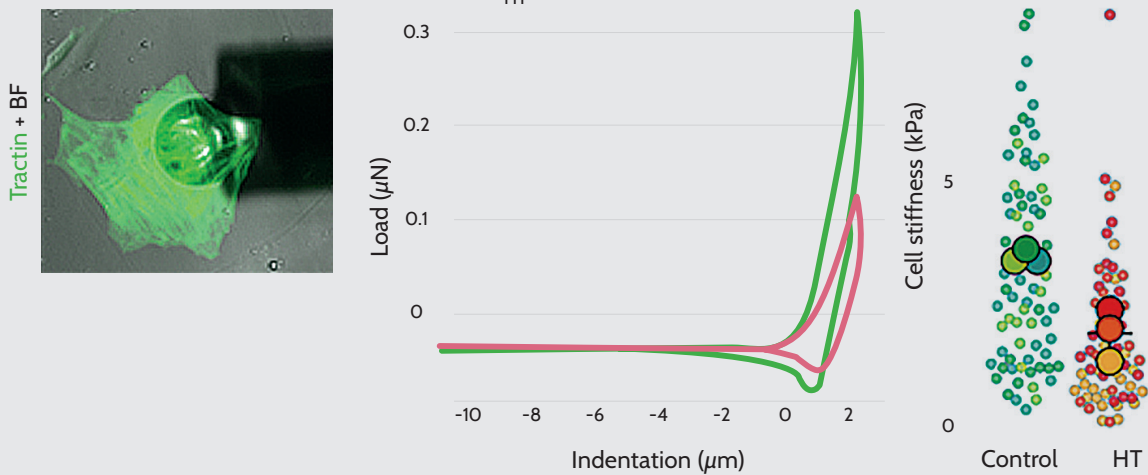
Their findings revealed that simulated blood pressure and stiffness independently influence the VSMC phenotype (Figure 2). However, only the combination of pressure and compliance leads to a complete phenotypic switch, including large-scale changes to mechanical properties, protein expression, cell morphology, actin organization, and the maximal formation of matrix-degrading podosomes. Additionally, single-cell pressure stimulation with a single indentation demonstrated a consistent increase in intracellular Ca2+ levels that could induce podosome formation, unveiling the mechanistic link between pressure changes and phenotypic alterations. Overall, this study emphasizes the significant impact of the mechanical environment on VSMC behavior with Optics11 Life technology, which influences the development of atherosclerosis.

Delving into the mechanics of specific subcellular compartments, Moch et al.[9] investigated how mechanical stress affects desmosome cell junctions by probing cell-cell contact areas at the edge of cell colonies with nanoindentation. They inactivated the actomyosin system in human keratinocytes (HaCaT) by low-dose treatment with the myosin II inhibitor para-nitro-blebbistatin and then monitored changes in desmosomal protein turnover. They assessed whether myosin II inhibition altered the elasticity of HaCaT cells.
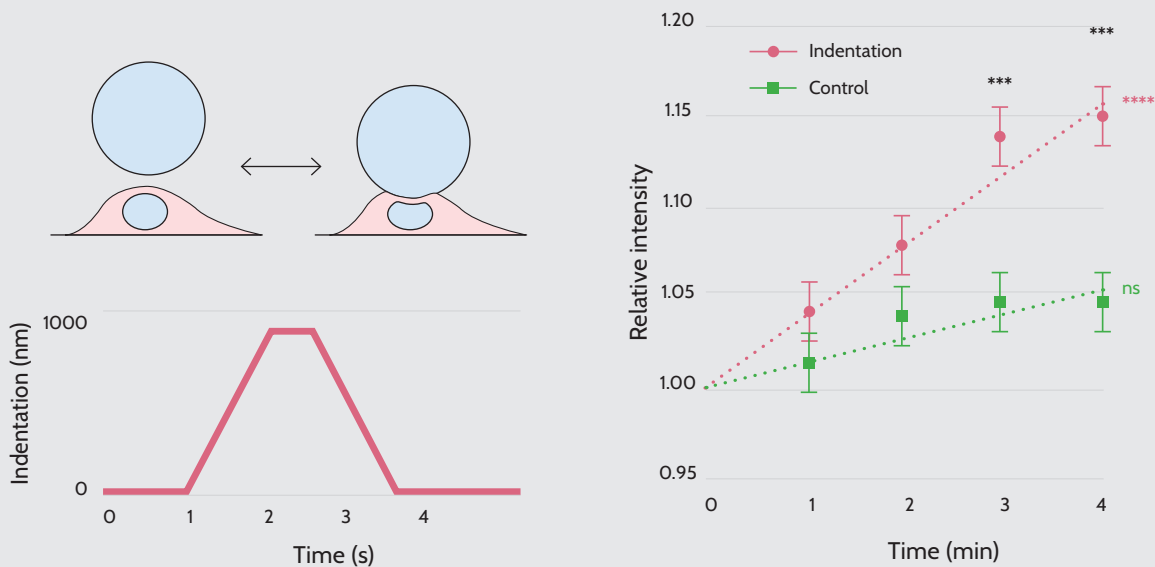
The results indicated that myosin II inhibition led to a decrease in Young's modulus at the cell-cell contact areas, and this reduction is dependent on the concentration of the drug (Figure 3). Furthermore, mechanical changes led to a reduction in desmosomal protein turnover. With the aid of Optics11 Life technology, these findings reveal desmosomes' capacity to sense and respond to mechanical signals, potentially impacting the mechanical properties of tissue.

A

* Compared to 1kPa of same group
* Compared to stiffness-matched control
* Compared to to stiffness-matched NBP

B NANOINDENTATION
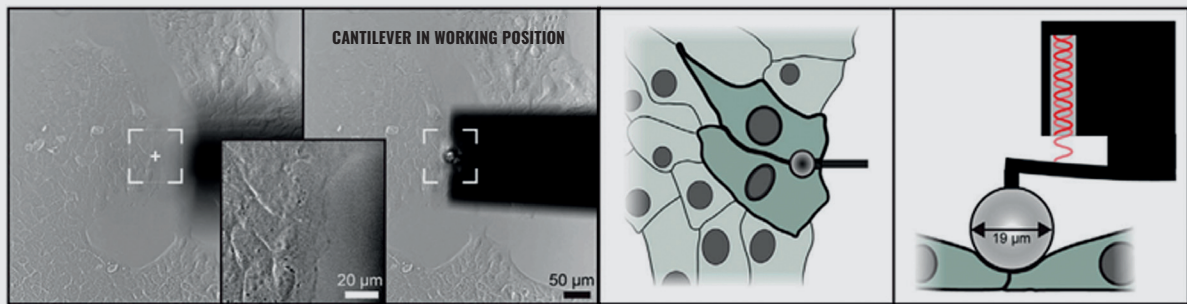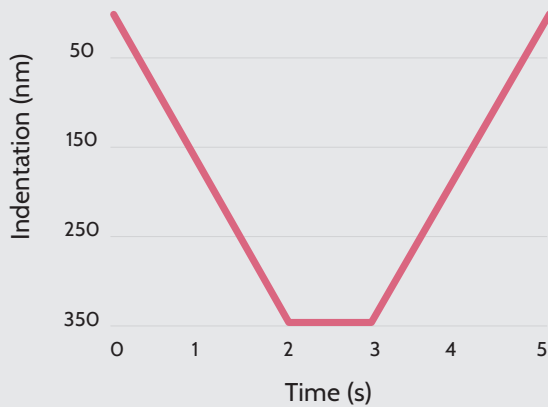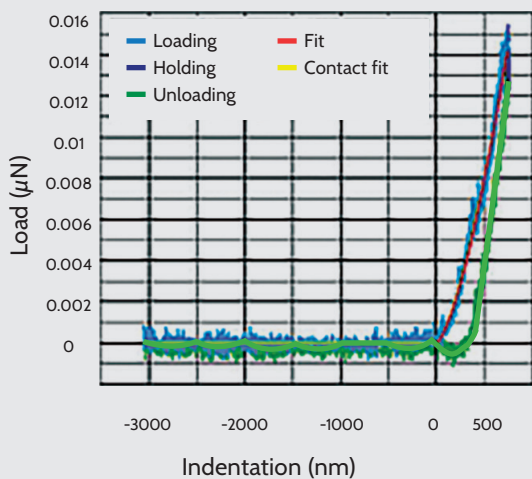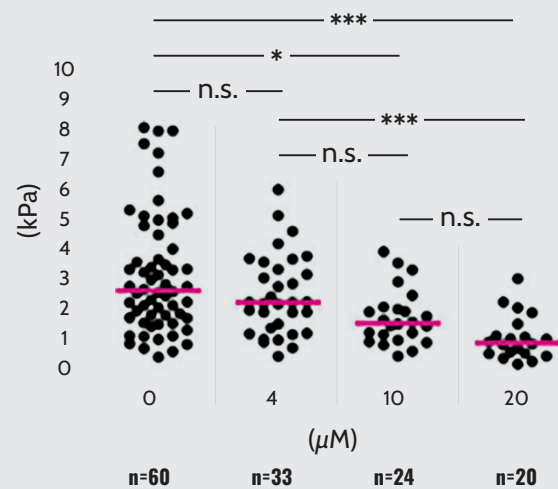
Tractin + BF

— Control
— HT

C

^ **Figure 2**

Figure 2 The impact of the local mechanical environment on single cells. **(A)** Percentage of podosome-forming cells in normal blood pressure (NBP) and systolic hypertension (HT) conditions. **(B)** Cellular stiffness after HT treatment and schematic of single cell indentation. **(C)** Pressure application with the nanoindenter. Ca2+ levels within VSMCs after a single indentation.

A

CANTILEVER IN WORKING POSITION

20 μm   50 μm   19 μm

B INDENTATION PROTOCOL

Indentation (nm): 50, 150, 250, 350
Time (s): 0, 1, 2, 3, 4, 5

C LOAD-INDENTATION PLOT

Load (μN): 0, 0.002, 0.004, 0.006, 0.008, 0.01, 0.012, 0.014, 0.016

Legend: Loading, Holding, Unloading, Fit, Contact fit

Indentation (nm): -3000, -2000, -1000, 0, 500

D EFFECTIVE YOUNG'S MODULUS

(kPa): 0, 1, 2, 3, 4, 5, 6, 7, 8, 9, 10

***
*
n.s.
***
n.s.
n.s.

(μM): 0, 4, 10, 20

n=60   n=33   n=24   n=20

^ Figure 3

Effects of para-nitro-blebbistatin treatment on HaCaT cell elasticity. **(A)** Left: bright-field images showing the positioning of the cantilever to the cells before and during indentation, noting that the cantilever is positioned at the border between two cells on the periphery of a cell colony. Right: schematic representations of the positioning of the cantilever from the top and the side, respectively. **(B)** Graph depicting the indentation protocol. The depth of indentation of 350 nm is reached in 2 seconds and held for 1 second, after which the probe is retracted at the same speed of indentation. **(C)** Load-indentation curve, displaying the loading, holding, and unloading phases. **(D)** Young's modulus for cells treated with 0, 4, 10, and 20 μM para-nitro-blebbistatin.

Note. Adapted from "Cortical tension regulates desmosomal morphogenesis", by Moch, M., 2022, Front Cell Dev Biol, 10:946190. doi: 10.3389/fcell.2022.946190.[9]

3D MULTICELLULAR SYSTEMS: FROM THE MICRO- TO MACROSCALE

The increased popularity of 3D cell cultures is largely attributed to their ability to closely resemble in vivo conditions and provide more physiologically relevant *in vitro* models. 3D cell culture systems significantly influence cell structure and mechanotransduction compared to traditional 2D monolayer culture setups. The mechanical response in 3D cell culture results from the properties of individual cells and the intricate interplay among these cells and the surrounding environment across various length scales, from micro- to macroscale[10]. Consequently, characterizing the mechanical properties of 3D multicellular systems becomes challenging, especially at micro-length scales where network complexity and cellular mechanics interact. Additionally, 3D systems can be composed of different cell types and exhibit variations in extracellular matrix (ECM) composition that lead to spatial heterogeneity in local mechanical responses[2,3].

Recent studies have demonstrated the impact of cell-matrix interactions and the mechanical properties of the ECM on 3D *in vitro* models[11,12,13,14]. Variations in ECM topography, stiffness, and deformability can significantly modify mechanical tension, impacting cellular processes. Therefore, an understanding of the composition and structure of the ECM is critical for the development of advanced 3D cultures.

Therefore, investigating the mechanical properties of tissue-derived ECM is essential for designing suitable 3D *in vitro* models that replicate tissue's multicellular nature and complex physiological microenvironments. In this context, Optics11 Life technology proves instru-mental in mapping the local mechanical properties of heterogeneous biological materials and elucidating their relationship to their overall mechanical behavior.

In view of the importance of extending the current knowledge of ECM mechanics, van Tienderen et al.[15] mechanically characterized the ECM of hepatocellular carcinoma (HCC) and cholangiocarcinoma (CCA) tumors at the microscale using nanoindentation. Their study introduced an ECM decellularization method to set up physiologically relevant 3D *in vitro* models. The decellularized scaffolds underwent microscale characterization by probing square matrices of 10 X 10 points separated by 100 μm.

Their findings reveal that ECM exhibits tumor-specific microscale mechanical properties. They observed a high level of heterogeneity among the scaffolds, with CCA-decellularized ECM providing the highest effective Young's modulus (Figure 4A). Interestingly, CCA and HCC showed a high level of patient-to-patient heterogeneity in tumor-derived and adjacent tissue-derived samples (Figure 4B). Additionally, the authors generated a heat map by plotting Young's modulus values over a 1 mm x 1 mm area per scaffold, thereby retaining information on their spatial location and heterogeneity (Figure 4C). They concluded that the development of CCA significantly affected the mechanical properties of the ECM. This study is a clear example of how mechanical characterization of the ECM using Optics11 Life technology can inform the design of mechanically relevant scaffolds to support 3D cultures in disease modeling.
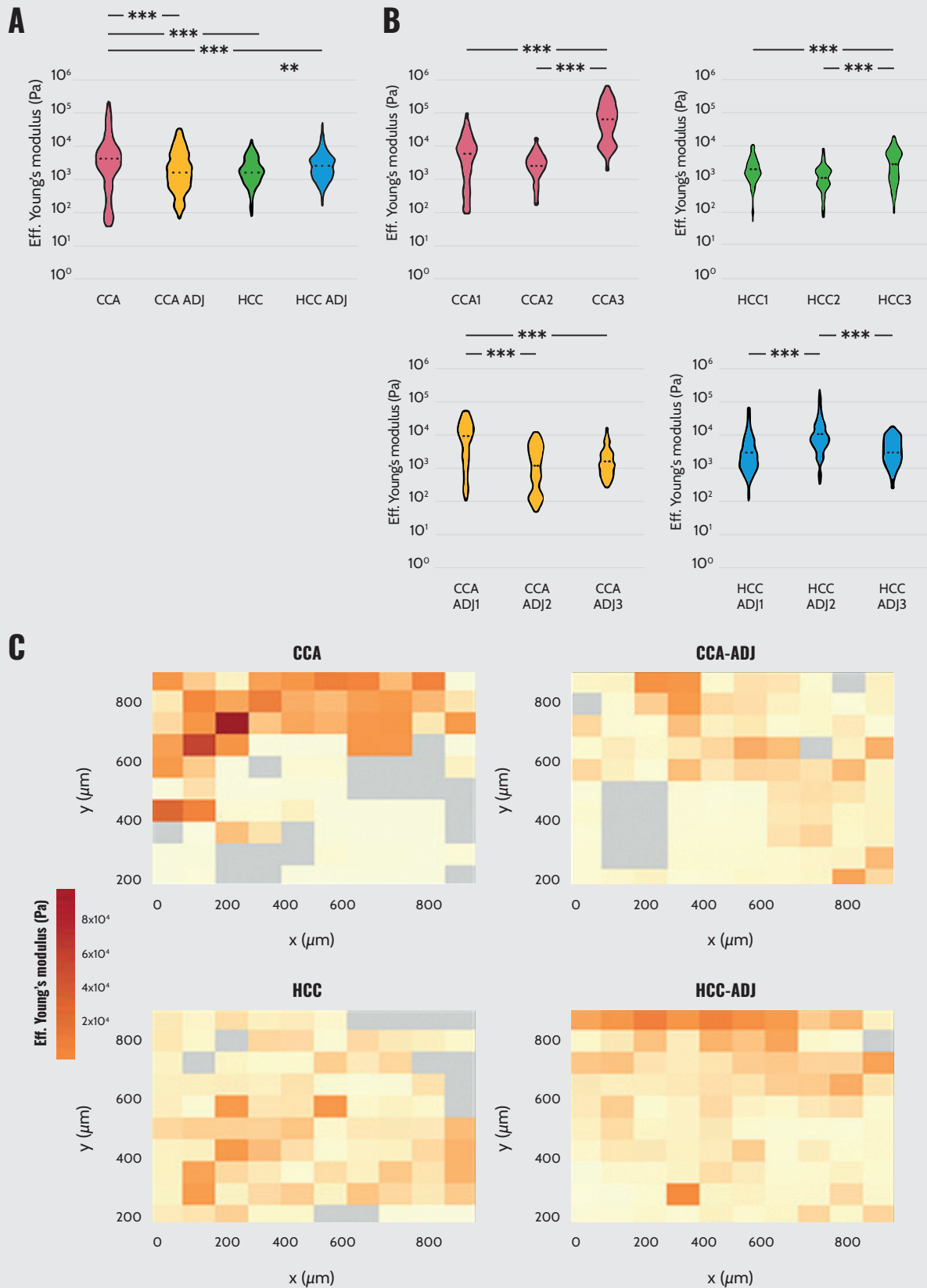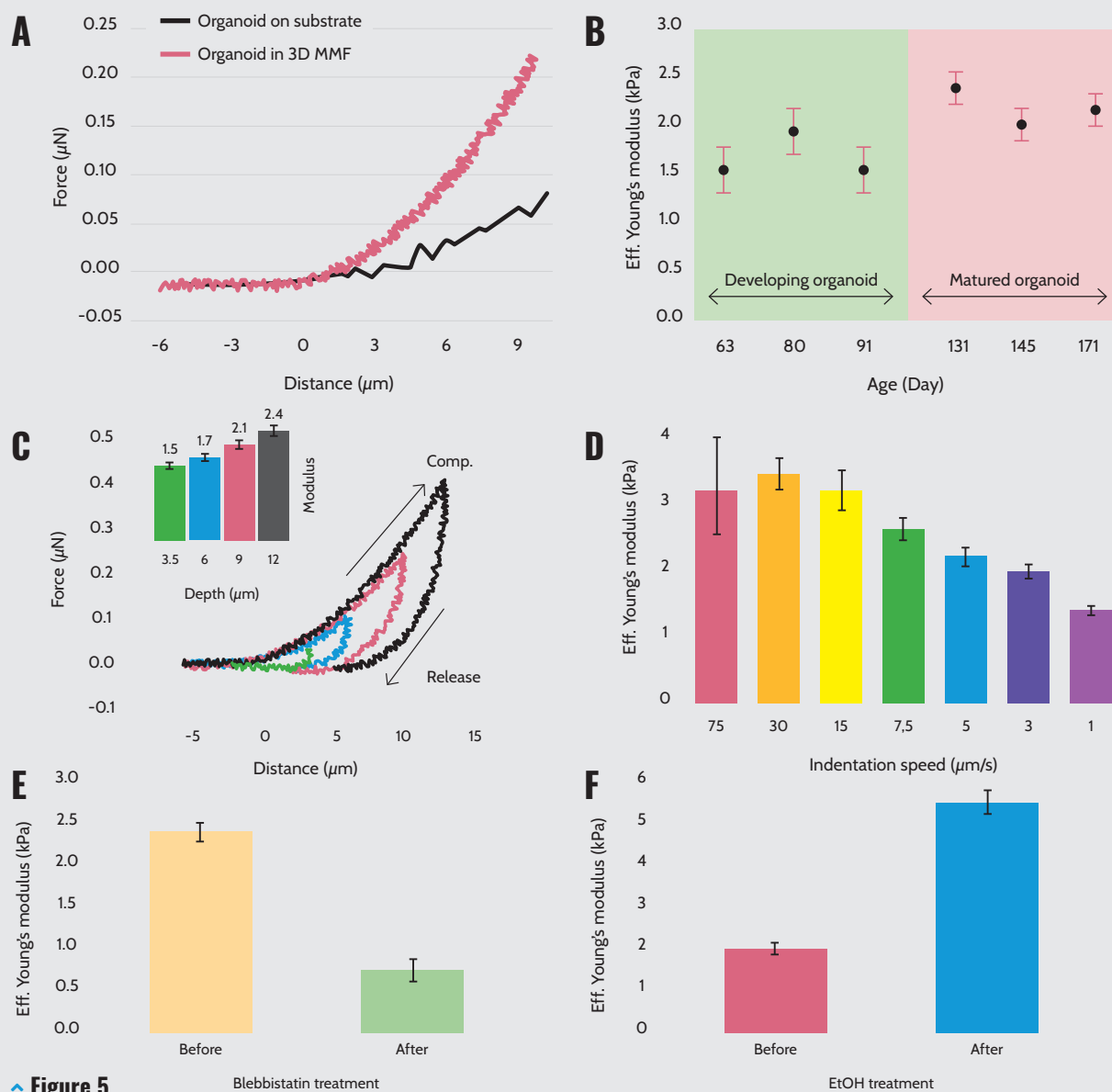
⌃ Figure 4

Mechanical characterization of decellularized scaffolds. **(A)** Violin plot visualizing the Effective Young's modulus for the different decellularized scaffolds: cholangiocarcinoma (CCA), hepatocellular carcinoma (HCC), CCA-adjacent tissue (ADJ), and HCC-ADJ. **(B)** Violin plot visualizing the effective Young's modulus per patient, displaying patient heterogeneity. **(C)** Representative heat maps of the Effective Young's modulus distribution in decellularized scaffolds.

Note. Adapted from "Tumor decellularization reveals proteomic and mechanical characteristics of the extracellular matrix of primary liver cancer", van Tienderen, G.S., 2023, Biomater Adv., 146:213289. doi: 10.1016/j.bioadv.2023.213289.[15]

Turning their attention directly to the mechanics of 3D multicellular structures, Ryu et al.[16] applied nanoindentation to cerebral organoids. To improve measurement accuracy, they designed 3D mesostructures to immobilize freestanding organoids mechanically and reversibly without damaging them. Figure 5A highlights the mechanical properties of cerebral organoids held in 3D mesostructures while immersed in cell culture media. The Effective Young's moduli determined from these measurements depend on age (Figure 5B), indentation depth (Figure 5C), and indentation speed (Figure 5D). Also, changes in mechanical characteristics induced by controlled exposure to compounds known to influence cytoskeletal dynamics, such as blebbistatin and ethanol, demonstrate that this setup allows the sensing of induced mechanical changes (Figures 5E and 5F). Therefore, this study showcases the possibility of extensively and accurately characterizing the mechanical profile of organoids using Optics11 Life technology without causing damage to these delicate structures.

Figure 5

Mechanical properties of cerebral organoids within 3D mesostructures. **(A)** Force-distance curves of organoids indented on the substrate and within the 3D multifunctional mesoscale frameworks (MMF). **(B)** Effective Young's modulus of organoids at different ages measured in a 3D MMF with an indentation speed of 5 μm/s. **(C)** Force-distance curves and effective Young's modulus of organoids indented at a speed of 5 μm/s with varying depths of indentation. **(D)** Effective Young's modulus values at different indentation speeds to a depth of 12 μm. Effective Young's modulus values before and after exposure to **(E)** blebbistatin and **(F)** ethanol.

Note. Adapted from "Transparent, Compliant 3D Mesostructures for Precise Evaluation of Mechanical Characteristics of Organoids", Ryu, H., 2021, Adv Mater., 33(25):e2100026. doi: 10.1002/adma.202100026.[16]

# HETEROGENEITY AND MULTISCALE COMPLEXITY OF TISSUES

Biological tissues are complex assemblies of diverse cell types, extracellular matrix, and molecular components that contribute to the specific functions of each tissue type[17]. Changes in tissue microstructure determine its mechanical properties, which may vary with age, disease development, and physiological status. Due to the heterogeneity and multiscale complexity of tissues, alterations in their mechanical properties occur at subcellular to cellular levels and at cellular to tissue levels[18]. In this sense, Optics11 life technology allows measuring the bulk mechanical properties over large tissue areas while providing high-resolution insights into tissue mechanical heterogeneities at a fine scale.

In a prime example of high-resolution large-scale characterization, Martinez-Vidal et al.[19] characterized the mechanics of the three tissue layers of the bladder (urothelium, lamina propria, and muscle layer) at a microscale level using nanoindention technology. They elucidated the mechanical alterations in the initiation and progression of actinic cystitis and bladder carcinoma in murine models.

The tissues were prepared by slicing the bladder wall tangentially to maintain the entire tissue (urothelium, lamina propria, and muscle layer) in each section. Acquisition points were separated by 10 μm to obtain a highly resolved map 100 μm wide and of sufficient length to cover the entire thickness of the bladder wall (around 400 μm).

Their analyses revealed that the healthy bladder wall is a mechanically heterogeneous tissue (Figure 6A). Specifically, the stiffness gradually increases from the urothelium to the lamina propria and decreases at the muscle outer layer. In the actinic cystitis model induced via X-ray irradiation, increased deposition of a dense extracellular matrix in the lamina propria was associated with fibrotic tissue stiffening (Figure 6A). Intriguingly, tumor initiation and invasion were associated with increased tissue compliance in the bladder cancer model (Figure 6B). In addition, they characterized the micromechanical profile of the human bladder of a patient with muscle-invasive bladder cancer. Compared to non-neoplastic tissue, neoplastic tissue exhibited mechanical heterogeneity and softening (Figure 6C). Through this high-resolution micromechanical investigation with Optics11 Life technology, the study delineates the intrinsic mechanical heterogeneity of the layers of a healthy bladder compared to the mechanical perturbations associated with actinic cystitis and bladder neoplasia.

A
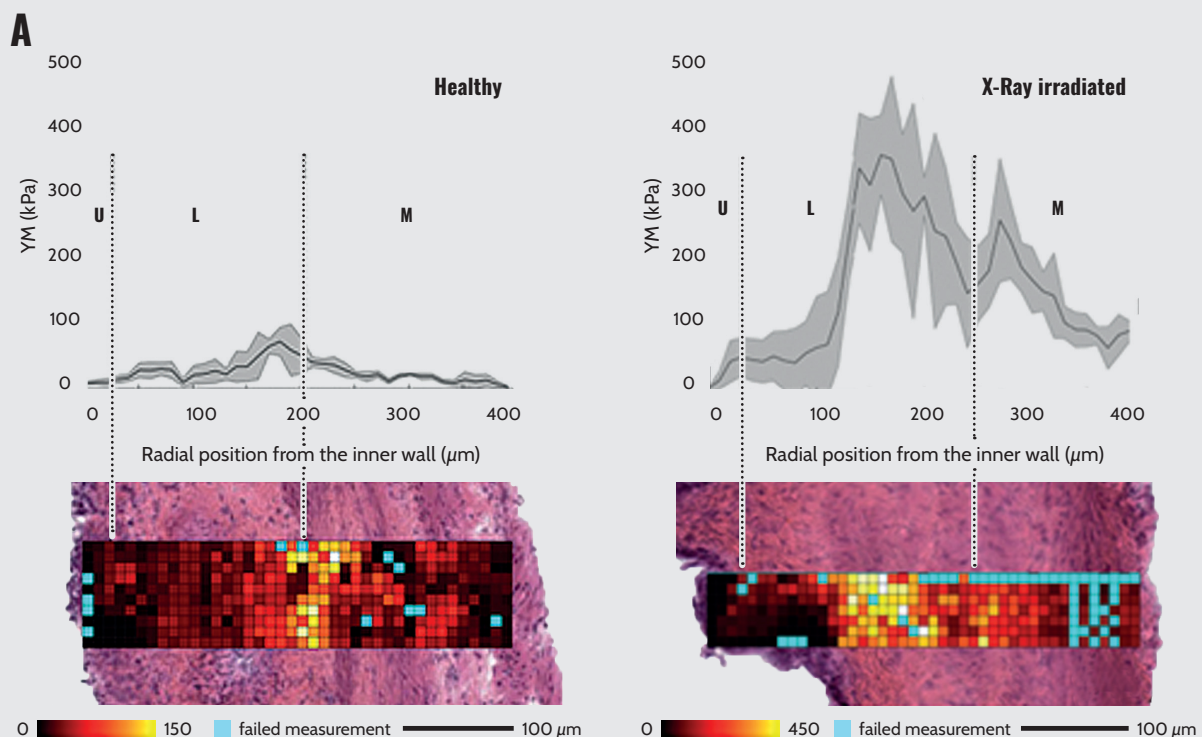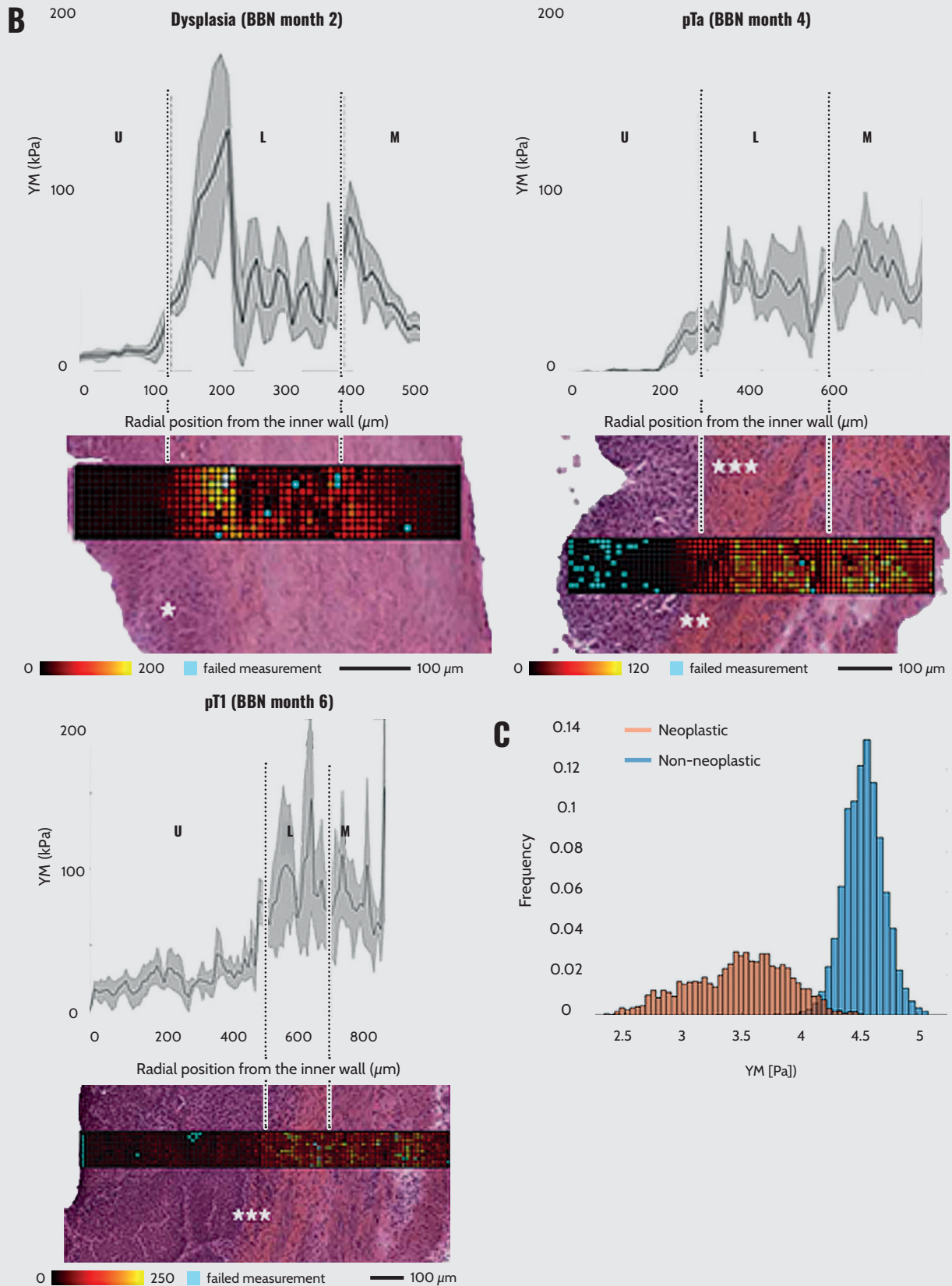
^ **Figure 6**

Micromechanics of bladders with nanoindentation. **(A)** Representative bladder wall stiffness gradient collected 4 months after treatment: X-rays cause a stiffening of the whole bladder wall compared to non-treated healthy animals. **(B)** Mechanical characterization of bladder wall stiffness after 2, 4, and 6 months of treatment with the bladder-specific carcinogen nitrosamine (BBN). U: urothelium, L: lamina propria, M: muscle. **(C)** Mechanical profile of neoplastic and non-neoplastic human muscle tissue.

Note. Adapted from "Micro-mechanical fingerprints of the rat bladder change in actinic cystitis and tumor presence", Martinez-Vidal, L., 2023, Commun Biol., 6(1):217. doi: 10.1038/s42003-023-04572-0.[19]

To characterize the microstructures and micromechanical properties of large tissue areas at high resolution, Leet et al.[20] combined nanoindentation and second-harmonic generation (SHG) microscopy to correlate cervical tissue stiffness with 3D collagen-fiber organization at the micrometer scale.

The cross-correlation of these results unveiled that the structural and mechanical properties are region-specific, and the elastic modulus measured from nanoindentation is strongly correlated with SHG parameters related to collagen concentration and dispersion of collagen-fiber orientation in 2D and 3D (Figure 7). In this study, Optics11 Life technology contributed to understanding the relation between collagen microstructure and tissue mechanics, knowledge that could be applied to improve disease detection methods.
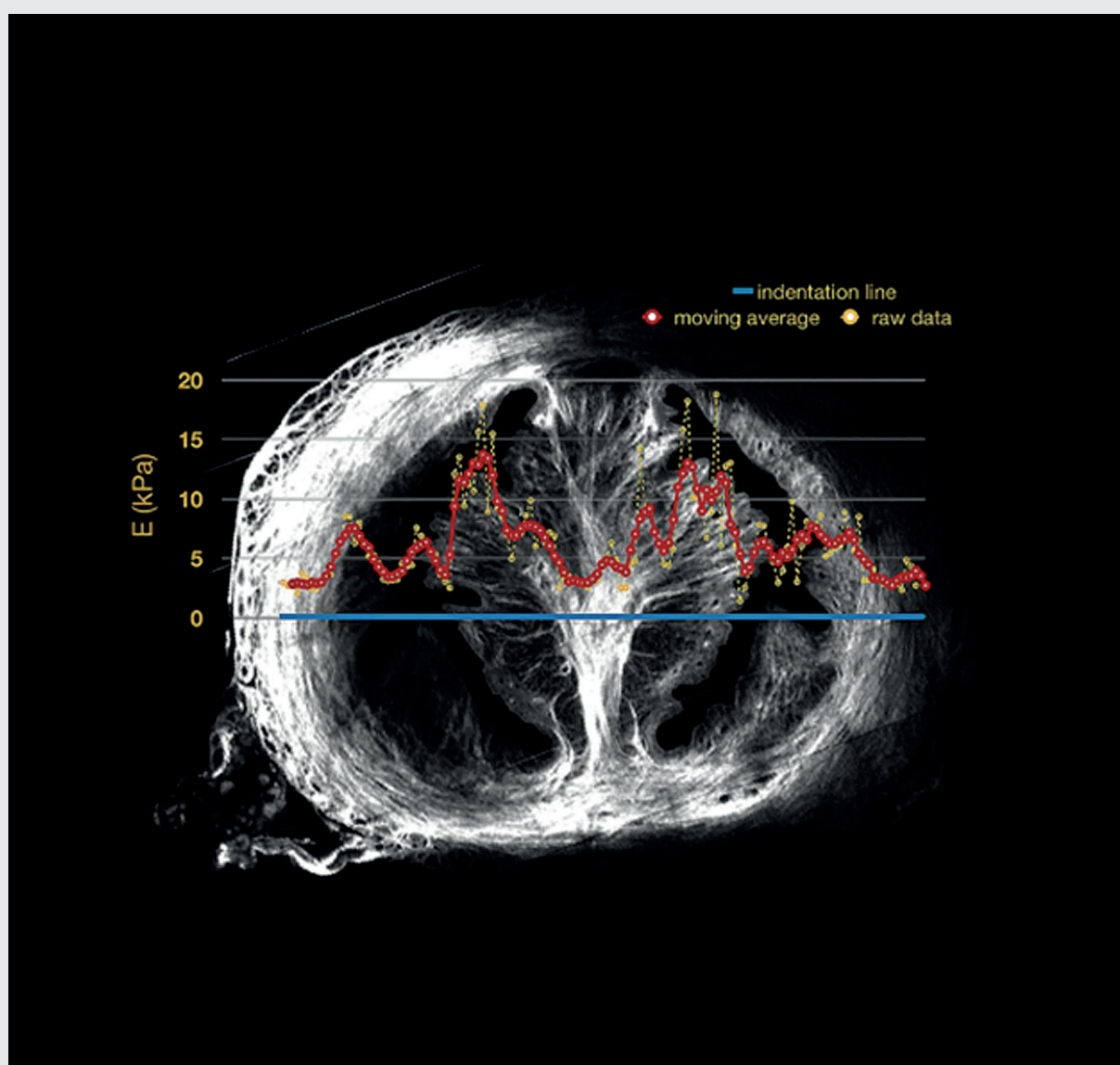
˄ Figure 7

Representative spatially heterogeneous mechanical properties and 3D microstructure of cervical tissue. Raw indentation data (yellow) and the moving average (red) of the indentation modulus are aligned with the blue line marking the indentation trajectory.

Note. Adapted from "An optomechanogram for assessment of the structural and mechanical properties of tissues", Lee, W., 2021, Scientifc Reports, 11:324. doi: s41598-020-79602-6.[20]

MICROSTRUCTURE AND MECHANICS OF BIOMATERIALS

Biomaterials used in medical implants, drug delivery systems, tissue engineering, and *in vitro* culture substrates must possess specific mechanical properties to ensure compatibility, functionality, and longevity. Properties such as strength, stiffness, density, composition, orientation, and viscoelasticity influence how biomaterials interact with biological systems[21]. Crucial challenges in using biomaterials, including hydrogels, are controlling cellular behavior, identifying mechanical triggers to initiate specific cellular activities, and creating 3D structures with properties similar to those of native tissues[22].

To reproduce the heterogeneity of the native ECM, Neves et al.[23] explored the influence of in-gel microstructures on the mechanical properties of alginate (ALG) hydrogels for cell delivery using nanoindentation. The ALG was modified with cyclooctyne groups to produce amphiphilic derivatives (ALG-K). This change allows ALG-K to form stable microstructures such as smooth hydrogels (low modification degrees, ALG-KL) or microstructured hydrogels (high modification degrees, ALG-KH). By comparing the spatial distribution of Effective Young's modulus (Eeff) between the two gels, the study showed that ALG-KH hydrogels are more heterogeneous than ALG-KL hydrogels (Figure 8). Dynamic mechanical analysis (DMA) further revealed that ALG-KL and ALG-KH hydrogels exhibited a similar average elastic modulus (E') of approximately 4 kPa and 3.2 kPa, respectively. The ratio of elastic (E') to viscous (E') components remained consistent between the two gels. However, the stiffest regions in ALG-KH hydrogels, corresponding to microstructures, were four times stiffer than the network's average value (E' ~12 kPa). These findings collectively suggest that the presence of in-gel microstructures significantly influences the mechanical heterogeneity within the hydrogels. Moreover, ALG hydrogels, as synthetic ECM, offer a unique platform for cell delivery. In this work, Optics11 Life technology was functional to retrieve accurate measurements of hydrogel mechanical properties, identify variations in stiffness, reveal viscoelastic behavior, and compare different hydrogel types, providing crucial information to guide hydrogel design for specific applications.
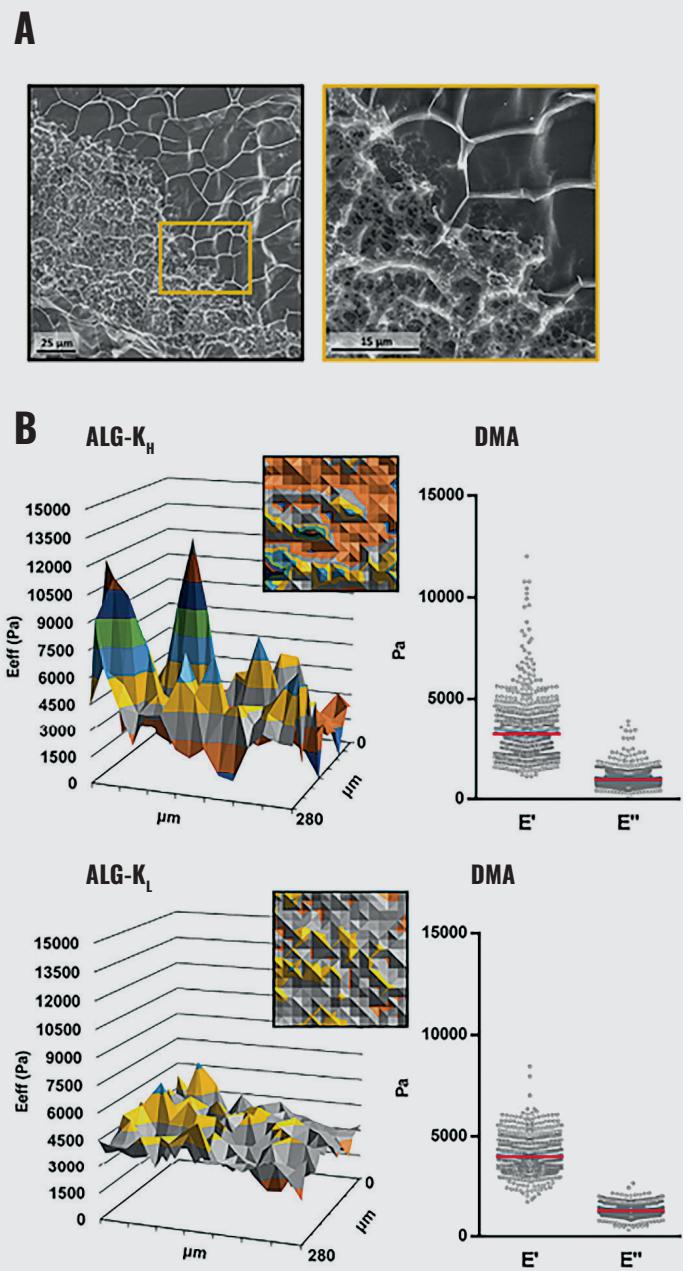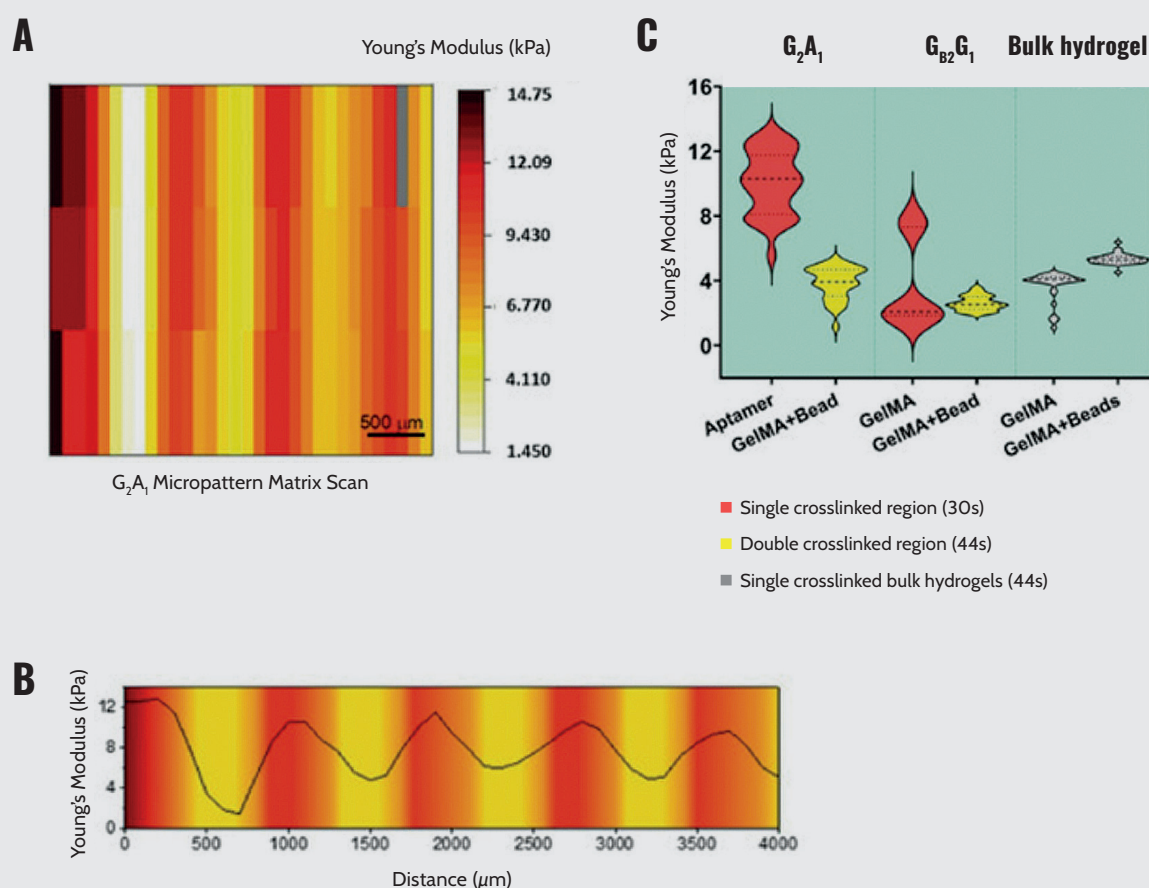
⌃ Figure 8

Characterization of ALG-K hydrogel's structural and mechanical heterogeneity **(A)** CryoSEM of ALG-KH hydrogels, showing distinct denser/loser regions. **(B)** Surface mechanical properties of ALG-KH (right) and ALG-KL hydrogels obtained by static (effective Young's modulus, Eeff) and DMA (elastic, E', and viscous, E", components) nanoindentation measurements.

Note. Adapted from "Microstructured click hydrogels for cell contact guidance in 3D", Neves, M.I., 2023, Mater Today Bio, 10;19:100604. doi: 10.1016/j.mtbio.2023.100604.[23]

Another study conducted by Rana et al.[24] demonstrated the micromechanical behavior of hydrogels in advanced growth factor-delivering systems to stimulate angiogenesis in tissue bioprinting applications. The system incorporates vascular endothelial growth factor (VEGF) within a 3D polymer, controlling its spatial and temporal availability to provide long-term support for angiogenesis and vascular remodeling processes. To that end, a two-step photolithography method was used to create micropatterns consisting of aptamer-functionalized gelatin methacryloyl (GelMA) that allow the binding of VEGF (referred to as the 'aptamer region') and pristine GelMA (referred to as the 'GelMA region'). The effect of aptamer incorporation on the stiffness of the gels was tested using nanoindentation.

The two-step photolithography process used in micropattern fabrication resulted in regions with different crosslinking densities. Specifically, the aptamer region underwent double crosslinking, whereas the GelMA region was single-crosslinked. The variation in crosslinking density had a significant impact on the micromechanical properties of the micropatterns. Consequently, the aptamer region exhibited a higher average Young's modulus compared to the GelMA region (Figure 9A). The differences in mechanical properties were not abrupt but showed a gradient across the micropatterns (Figure 9B). This gradient likely resulted from the two-step photocrosslinking process as well as the overlaying of the second pre-polymer onto the first crosslinked pattern.

Figure 9

Micromechanical behavior of bicomponent micropatterns. **(A)** Matrix scan of Young's modulus of the crosslinked micropattern, revealing the mechanical difference between the aptamer and GelMA regions. **(B)** Young's modulus quantification of different regions in photocrosslinked aptamer/GelMA micropatterns or bulk GelMA/GelMA mixed with fluorescent microbeads, revealing the effect of aptamer content on the extent of crosslinking. **(C)** Young's modulus profile across the long axis of a micropattern depicting the gradual variation in Young's modulus magnitude between regions.

Their results suggest that the incorporation of aptamers into the GelMA matrix influences the crosslinking density and mechanical modulus of the hydrogel (Figure 9C). Here, Optics11 Life technology provided precise measurements of the mechanical properties of micropatterns, revealed the influence of aptamer incorporation, and identified mechanical gradients in a 3D environment for vascular remodeling.

6   CONCLUSION

Optics11 Life instruments provide researchers with accurate, detailed, and comprehensive mechanical characterization of a variety of samples, including cells, subcellular compartments, 3D cultures, tissue sections, decellularized matrix, and biomaterials. The ability to measure the mechanical properties of relatively large areas at high resolution empowers scientists to gain a deeper understanding of the behavior and function of biological samples and biomaterials, representing a significant advancement in the field of mechanobiology.

DISCLAIMER

REFERENCES

1 **Kimura S, Tsuji T.** Mechanical and Immunological Regulation in Wound Healing and Skin Reconstruction. Int J Mol Sci. 2021 May;22(11):5474. doi: 10.3390/ijms22115474.

2 **Antonovaite N, et al.** Regional variations in stiffness in live mouse brain tissue determined by depth-controlled indentation mapping. Sci Rep. 2018 Aug 21;8(1):12517. doi: 10.1038/s41598-018-31035-y.

3 **van Hoorn H, et al.** Local dynamic mechanical analysis for heterogeneous soft matter using ferrule-top indentation. Soft Matter. 2016 Mar 28;12(12):3066-73. doi: 10.1039/c6sm00300a.

4 **Wu PH, et al.** A comparison of methods to assess cell mechanical properties. Nat Methods. 2018 Jul;15(7):491-498. doi: 10.1038/s41592-018-0015-1.

5 **Swaminathan V, Gloerich M.** Decoding mechanical cues by molecular mechanotransduction. Curr Opin Cell Biol. 2021 Oct;72:72-80. doi: 10.1016/j.ceb.2021.05.006.

6 **Chen J.** Nanobiomechanics of living cells: a review. Interface Focus. 2014 Apr;4(2):20130055. doi: 10.1098/rsfs.2013.0055.

7 **Darling EM, Di Carlo D.** High-Throughput Assessment of Cellular Mechanical Properties. Annu Rev Biomed Eng. 2015;17:35-62. doi: 10.1146/annurev-bioeng-071114-040545. Epub 2015 Jul 16. PMID: 26194428; PMCID: PMC8204286.

8 **Swiatlowska P, et al.** Pressure and stiffness sensing together regulate vascular smooth muscle cell phenotype switching. Sci Adv. 2022 Apr;8(15):eabm3471. doi: 10.1126/sciadv.abm3471.

9 **Moch M, at al.** Cortical tension regulates desmosomal morphogenesis. Front Cell Dev Biol. 2022 Oct 4;10:946190. doi: 10.3389/fcell.2022.946190.

10 **Boot RC, et al.** Spheroid mechanics and implications for cell invasion. Advances in physics. 2021; 6(1): 1978316. doi: 10.1080/23746149.2021.1978316.

11 **Giobbe GG, et al.** Extracellular matrix hydrogel derived from decellularized tissues enables endodermal organoid culture. Nat Commun. 2019 Dec;10(1):5658. doi: 10.1038/s41467-019-13605-4.

12 **Willemse J, et al.** Hydrogels derived from decellularized liver tissue support the growth and differentiation of cholangiocyte organoids. Biomaterials. 2022 May;284:121473. doi: 10.1016/j.biomaterials.2022.121473.

13 **van Tienderen GS, et al.** Modelling metastatic colonization of cholangiocarcinoma organoids in decellularized lung and lymph nodes. Front Oncol. 2023 Jan;12:1101901. doi: 10.3389/fonc.2022.1101901.

14 **van Tienderen GS, et al.** Extracellular matrix drives tumor organoids toward desmoplastic matrix deposition and mesenchymal transition. Acta Biomater. 2023 Mar;158:115-131. doi: 10.1016/j.actbio.2022.11.038.

15 **van Tienderen GS, et al.** Tumor decellularization reveals proteomic and mechanical characteristics of the extracellular matrix of primary liver cancer. Biomater Adv. 2023 Mar;146:213289. doi: 10.1016/j.bioadv.2023.213289.

16 **Ryu H, et al.** Transparent, Compliant 3D Mesostructures for Precise Evaluation of Mechanical Characteristics of Organoids. Adv Mater. 2021 Jun;33(25):e2100026. doi: 10.1002/adma.202100026.

17 **Johnston A, Callanan A.** Recent Methods for Modifying Mechanical Properties of Tissue-Engineered Scaffolds for Clinical Applications. Biomimetics (Basel). 2023 May;8(2):205. doi: 10.3390/biomimetics8020205.

18 **Akhtar R, et al.** Characterizing the elastic properties of tissues. Mater Today (Kidlington). 2011 Mar;14(3):96-105. doi: 10.1016/S1369-7021(11)70059-1.

19 **Martinez-Vidal L, et al.** Micro-mechanical fingerprints of the rat bladder change in actinic cystitis and tumor presence. Commun Biol. 2023 Feb;6(1):217. doi: 10.1038/s42003-023-04572-0.

20 **W. Lee, et al.** An optomechanogram for assessment of the structural and mechanical properties of tissues. Scientifc Reports. 2021;11:324. doi: s41598-020-79602-6.

21 **Ahearne M.** Introduction to cell-hydrogel mechanosensing. Interface Focus. 2014;4(2):20130038. doi: 10.1098/rsfs.2013.0038.

22 **Geckil H, et al.** Engineering hydrogels as extracellular matrix mimics. Nanomedicine. 2010;5(3):469-84. doi: 10.2217/nnm.10.12.

23 **Neves MI, et al.** Microstructured click hydrogels for cell contact guidance in 3D. Mater Today Bio. 2023 Mar;19:100604. doi: 10.1016/j.mtbio.2023.100604.

24 **Rana D, et al.** Spatial control of self-organizing vascular networks with programmable aptamer-tethered growth factor photopatterning. Mater Today Bio. 2023 Jan;19:100551. doi: 10.1016/j.mtbio.2023.100551.